Geomechanics and Engineering, *Vol. 32, No. 1 (2023) 35-47*
https://doi.org/10.12989/gae.2023.32.1.035

Geotechnical problems in flexible pavement structures design

Mato G. Uljarević*, Snježana Z. Milovanović, Radovan B. Vukomanović and Dragana D. Zeljić

Faculty of Architecture, Civil Engineering and Geodesy, University of Banja Luka, Bulevar Vojvode Stepe Stepanovića 77/3, Banja Luka, Bosnia and Herzegovina

(*Received December 28, 2021, Revised December 15, 2022, Accepted December 21, 2022*)

Abstract. Deformability of road pavements in the form of ruts represent a safety risk for road users. In the procedures for dimensioning the pavement structure, the requirement that such deformations do not occur is imperatively included, which results in the appropriate selection of elements (material, geometry) of the pavement structure. Deformability and functionality, will depend of the correct design of pavement structure during exploitation period. Nevertheless, there are many examples where deformations are observed on the pavement structure, in the form of rutting at parts of the road with relatively short length, realised in the same climatic and the same geoenvironmental conditions. The performed analysis of deformability led to the conclusion that the level of deformation is a function of the speed of traffic. This effect is observed on city roads, but also outside of urban areas at roads with speed limits are significant, due to the traffic management, traffic jams (intersections, etc.). Still, the lower speed cause greater deformations. The authors tried to describe the deformability of flexible pavement structures, from the aspects of geotechnical problems, as a function of driving speed. Outcome of the analysis is a traffic load correction coefficient, in terms of using the existing methods of flexible pavement structures design.

Keywords: creep; flexible pavement structure; geotechnical problems; traffic load; traffic load correction coefficient

1. Introduction

Modern flexible pavement structures are multi-layer construction that consist of bitumen-bound materials - asphalt course and aggregate base course. The base course consist of unbound granular rock material, bound granular stone material with a appropriate type of binder or a combination of these materials. The behavior of pavement structure layers under traffic load and other influences (temperature, humidity) is complex. Experience indicates that the durability of the pavement is greatly influenced by the type of subgrade (soil) under pavement structure as well as from traffic load. Gomes Correla and Ramos (2021) proposed a geomechanical classification of the substrate based on stiffness and permanent deformations estimated using a triaxial test. Schulz-Poblete *et al.* (2018) presented the influence of humidity change on the deformation properties of materials in railway infrastructure. The first methods of pavement dimensioning, developed in the 1930s, were based on the acquired experiences and observations of existing pavements, and included a small number of influential parameters. Later, these methods were improved, but the real basis for the development of reliable methods for pavement dimensioning was laid by making test road sections (AASHTO Road Test, 1960s) (AASHTO 1972). Based on these tests, appropriate data were obtained and practical methods ("empirical methods") were developed, for asphalt pavement dimensioning. These methods are relatively simple to apply and provide the reliable design of pavements because it is actually a reproduction of previously verified results. However, these methods do not provide insight into stress and strain state, and deformation in pavements exposed to traffic load and other influences. In addition, the basis of these methods are pavement systems and materials applied in the AASHTO Road Test. Recently, theoretical design methods through which materials of any properties can be checked as well as any applied systems of pavements have been introduced in practice. Theoretical methods are based on the classical engineering principle of stress-strain calculation in characteristic-critical sections and their comparison with permissible values of these phenomena (Cvetanović and Banić 2007). The design of pavement structures is a very complex process where there are two groups of problems, namely, problems of design of construction and problems of material properties conversance. Under certain conditions (new pavements, short-term load, usual temperatures), it is acceptable the assumption of elastic behavior of the material in the pavement structure. Many methods for calculations of pavements have been developed on this assumption. Several authors have contributed to the method of calculation based on the theory of elasticity. Burmister's solutions (1943, 1945) are still the basis for nowadays calculations. Since the calculations according to the basic solutions are very complex, auxiliary tools (tables, nomograms) have been developed to define stresses in a simpler way. Nowadays, a large number of softwares have been developed, which has made it much easier to work on the design of pavement structures, and has achieved greater reliability of the calculation.

In first step of pavement design it is common to use empirical methods, and then stresses and strains in the

*Corresponding author, Professor
E-mail: mato.uljarevic@aggf.unibl.org

ISSN: 2005-307X (Print), 2092-6219 (Online)

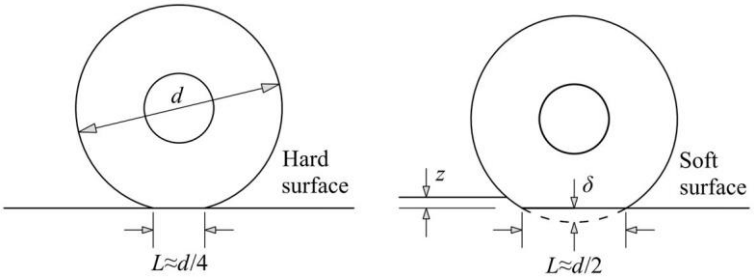

Fig. 1 Contact lengths of tires on hard and soft surfaces, adapted from McKyes (AASHTO 1972)

characteristic cross-sections of the pavement previously adopted using empirical methods are controlled by theoretical methods. The composition, thickness and arrangement of layers for certain types of flexible pavements depend mostly on the traffic load, soil-subgrade properties and climatic-hydrological conditions. Depending on the application and combination of certain types of materials and their quality, the composition of flexible pavements in principle differs according to the type of substrate under the bitumen-bound materials in surface course. A very large number of parameters that affect the design of pavement thickness require careful analysis and accurate calculation. Unlike previous procedures that used empirical assumptions and maximal simplifications of this otherwise complex problem, the aim of modern procedures is to establish the most accurate physical connection, and thus mathematical connection, of all parameters that affect the thickness, durability and resistance of the pavement, as well as on construction and maintenance costs.

Pavement structures design is a very delicate discipline in road design. Nowadays, around the world there are several methods for design of pavemens, and they are based on the results of AASHTO experiments performed in the state of Illinois in 1959 and 1960. The first design instructions of the association for public roads and transport – AASHTO (The American Association of State Highway and Transportation Official) was published in 1961 and since then, amendments have been published regularly, which follow the latest knowledge in the field of pavement construction. Relevant parameters for pavement design are: exploitation period to first strengthening, design period, traffic load, environmental impact, quality criteria, material characteristics, characteristics of pavements.

2. Traffic load

The traffic load is caused by the action of vehicles moving on the pavement or standing on it. The load is transferred to the pavement via wheels (tires) whose number depends on the type of vehicle and the number of axles (Babić 1997). The impact of traffic load was examined in detail in the USA through the AASHTO Road test, which included asphalt (flexible) and concrete (rigid) pavement structures. By processing the data obtained by the AASHTO experiment, we see that the pavement is affected by the axle loads and the number of load applications. The damage effect of the axle of 82 *kN* (represents the standard American axle) is taken, which is marked with the damage factor (equivalence factor), f=1, while all other, lighter or heavier axles, have their factors greater or less than one, $f \neq 1$. A larger number of load applications cause more damages at the pavement structure. The number of axle load transitions affects the selection of pavement structure.

The traffic load, or the number of axle passes can be expressed as the average daily traffic load and as the total traffic load in the design period. In order to adequately determine the traffic load, we use the traffic forecast from which we get the number of axle passes on a certain section. These axles are also called equivalent axles. When analyzing the traffic load we take into account: average annual daily number of heavy vehicles in the planned initial year of road use, average annual growth rate of the number of heavy vehicles in the design period, axle load of representative vehicle types, average capacity utilization of heavy goods vehicles, and distribution of traffic load on traffic lanes.

The load is transferred to the pavement via wheels (tires) whose number depends on the type of vehicle and the number of axles. The flexible tire has a smaller contact area on a hard surface than it does on soft surface. The rule that can be used to estimate the tire contact area is shown by Eq. (1) (Rashidi *et al.* 2013)

$$A = b \cdot L \tag{1}$$

where A is tire contact area (m^2), b is width of tire (m) and L is contact length of tire (m). An approximate method for estimating contact length of tire on hard and soft surfaces (see Fig. 1) is $L=d/4$ (on a hard surface) and $L=d/2$ (on a soft surface), where d is overall diameter of unloaded tire (m) (Babić 1997).

The main assumption when designing a pavement structure is that the vertical stress at the contact of the pavement and the tire is equal to the pressure in the tire and that it is in circular and uniform shape (De Beer *et al.* 2012). Comparing data from worldwide surveys, it is observed that the average pressure has increased by 20% over 20 years, apparently due to the improved design of tires for heavy trucks and tire durability (Shayesteh *et al.* 2017). The width of the tire will depend on the pressure in the tires (Burmister 1943). As the tire pressure increases, the aggressiveness on the pavement increases too (Huhtala *et al.* 1989). At the level of total road deflections, double tires damage the pavement less than wide tires (Huhtala *et al.* 1989, Pascale *et al.* 2011). Smaller double tires are more aggressive than normal size double tires (Huhtala *et al.* 1989).

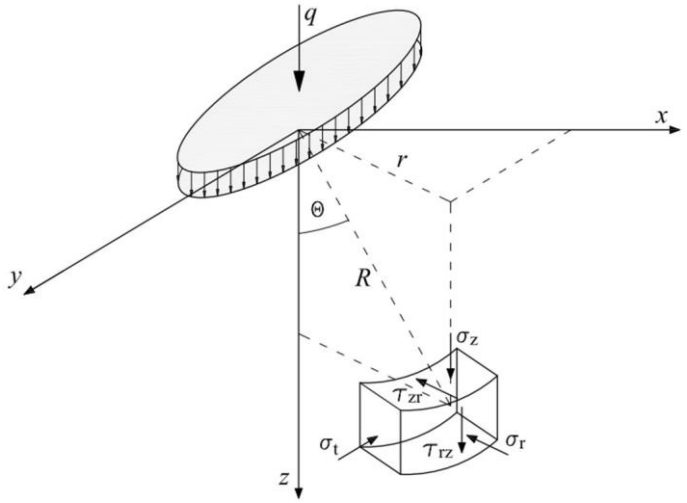

Fig. 2 Stress components under axisymmetric loading

3. Stress-strain state in the pavement construction caused by traffic load

The simplest way to perceive the behavior of a flexible pavement structure under load is to view it as a homogeneous half-space. A half-space is an infinitely large volume of soil that is bordered on the upper side by a plane on which the load is located. The original Boussinesq theory (1885), (Ullidtz 1997) was based on the concept of concentrated loading on an elastic (E, v), homogeneous and isotropic half-space. Stresses, dilatations (deformations) and deflections were performed to satisfy the circular surface under concentrated load. Before Burmister (1943) developed layer theory, much attention was paid to this Boussinesq solution, as it was the only one available. This theory can be used to determine stresses, dilatations and deflections in the subgrade, if the modulus coefficient between the bearing layer and the subgrade is close to one, as shown on a thin asphalt layer laid over a thin bearing layer of unbound aggregate. If the modulus coefficient is significantly greater than one, then the equation must be modified, as shown in the old Kansas State Highway Commission procedure (1947).

Fig. 2 shows a homogeneous half-space exposed to a circular evenly distributed load q over a surface of radius a. The half-space has a modulus of elasticity E and a Poisson's ratio v. Due to the characteristics of axial symmetry, three normal stresses σ_z, σ_r, σ_t, and one shear stress τ_{rz} equal to τ_{zr} act on a small cylindrical element with the center at a distance z below the surface and a radius r from the axis of symmetry. These stresses are functions of q, r/a and z/a.

When a load is applied over a circular elastic surface, the most critical stresses, dilatations, and deflections occur below the center of the loaded surface, in the axis of symmetry (Huang 1993). Then $\tau_{rz}=0$, $\sigma_r=\sigma_t$, so that σ_z and σ_r are the main stresses (the disposition is shown in Fig. 2).

$$\sigma_z = q \cdot [1 - \frac{z^3}{(\sqrt{a^2 + z^2})^3}] \tag{2}$$

$$\sigma_r = \frac{q}{2} \cdot [1 + 2 \cdot \nu - \frac{2 \cdot (1+\nu) \cdot z}{\sqrt{a^2 + z^2}} + \frac{z^3}{(\sqrt{a^2 + z^2})^3}] \tag{3}$$

$$\varepsilon_z = \frac{(1+\nu) \cdot q}{E} \cdot [1 - 2 \cdot \nu - \frac{2 \cdot \nu \cdot z}{\sqrt{a^2 + z^2}} - \frac{z^3}{(\sqrt{a^2 + z^2})^3}] \tag{4}$$

$$\varepsilon_r = \frac{(1+\nu) \cdot q}{2 \cdot E} \cdot [1 - 2 \cdot \nu - \frac{2 \cdot (1-\nu) \cdot z}{\sqrt{a^2 + z^2}} - \frac{z^3}{(\sqrt{a^2 + z^2})^3}] \tag{5}$$

$$w = \frac{(1+\nu) \cdot q \cdot a}{E} \cdot \left[\frac{a}{\sqrt{a^2 + z^2}} + \frac{1 - 2 \cdot \nu}{a} \cdot (\sqrt{a^2 + z^2} - z) \right] \tag{6}$$

where q is distributed load from tire pressure, a is contact surface radius, z is vertical coordinate, v is Poisson's ratio, E is modulus of elasticity of the layer, σ_z is vertical stress at depth z, σ_r is radial stress (tensile stress), ε_z is vertical dilatation at depth z, ε_r is radial dilatation (tension dilation), w is vertical displacement. On the surface of the half-space, the vertical displacement is

$$w_o = \frac{2 \cdot (1 - \nu^2) \cdot q \cdot a}{E} \tag{7}$$

Boussinesq solutions are based on the assumption that the half-space is composed of a linearly elastic material. It is well known that the materials in the subgrade are inelastic and are characterized by instantaneous deformation under stationary load. However, under the application of repeated traffic loads, most deformations are reversible and can be considered elastic. That is why it is possible to connect reasonable elastic modules with the speed of load movement. Since linearity implies the application of the superposition procedure, the elastic constant must not vary with the stress state. In other words, the uniaxial deformation of a linearly elastic material under uniaxial stress should be independent of the limited lateral pressure. This is obviously not true for earthen materials, because their axial deformation strictly depends on the magnitude of the limited lateral pressure. As a consequence, the

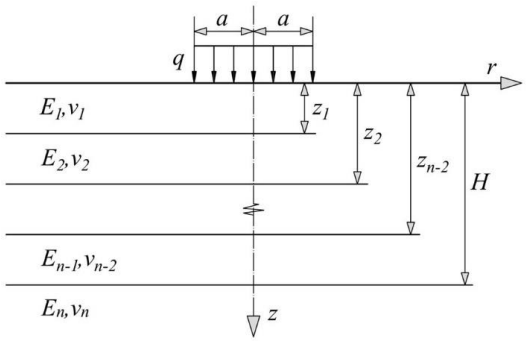

Fig. 3 Calculation model for a system with *n* layers

nonlinearity effects of the Boussinesq solution are of practical interest. Flexible pavements are layered systems with better materials in the upper layers and in no way represent a homogeneous half-space. Therefore, the use of Burmister's layer theory is more appropriate. Burmister (1943) first developed a two-layer system and then developed it into a three-layer system (Burmister 1945). With the development of computer technology, this theory can be applied to multilayer systems. This was applied by Huang (1967, 1968a), where the number of layers is infinite. Fig 3. shows a system with *n* layers.

Elastic-viscoelastic appropriate principles can be applied; directly on moving loads for determining surface deflections on a viscoelastic half-space (Perloff and Moavenzadeh 1967); for stresses and displacements in a two-layer viscoelastic system (Chou and Larew 1969); in a three-layer system, (Elliot and Moavenzadeh 1971); in a multi-layer system (Huang 1973b). The simplified method was applied in the computer program VESYS and KENLAYER.

Vertical stresses at the top of the subgrade are a significant factor in the dimensioning of pavement structures. The role of the pavement structure is to reduce the vertical stresses on the subgrade, so that harmful deformations of the structure are avoided. Huseyin Boler *et al.* (2018) used advanced instrumental methods and numerical modeling in the analysis of rutting substructure in several real problems. Thu Le *et al.* (2015) presented predictions of settlement of thick layers of soft clay using the parameters provided by numerical analysis of nonlinear creep in the elasto-visco-plastic model. Kim *et al.* (2009) analyzed flexible pavement structures by nonlinear modeling using three-dimensional finite elements. The allowable vertical stress on a particular subgrade depends on the strength or modulus of the subgrade. Combining the effects of stress and strength, vertical expansion due to pressure is the most common criterion for dimensioning. This simplification applies to highways and airport runways, because vertical expansion is primarily caused by vertical stress, while the effects of horizontal stress are relatively small.

The allowable vertical pressure depends on the number of load repetitions. Based on the dimensioning criteria according to the Shell method and based on the AASHTO equation, (Huang *et al.* 1984b) developed the following relation

$$N_d = 4.873 \cdot 10^{-5} \cdot \left(\frac{\sigma_c}{6.9}\right)^{-3.734} \cdot \left(\frac{E_2}{6.9}\right)^{3.583} \quad (8)$$

where N_d is allowed number of load repetitions to limit permanent deformation, σ_c is vertical stress pressure on the surface of the subgrade [kPa] and E_2 is modulus of elasticity on the subgrade [kPa].

4. Geo-substrate deformations depending on load duration

The effect of the load is felt by the soil usually to a depth of about two to three times the width of the loaded surface. The soil within this depth becomes compressed due to the imposed stresses. Compression of the soil mass leads to a decrease in the volume of the mass, which results in settlement of the structure. Compression of soil mass caused by imposed stresses can be almost instantaneous or temporal, depending on the characteristics (with respect to permeability) of the soil. Non-cohesive soils, which are very permeable, are compressed in a very short period of time compared to cohesive soils, which are less permeable.

The compressibility of the soil mass mainly depends on the stiffness of the soil skeleton. Stiffness, on the other hand, depends on the structural arrangement of the particles and, in fine-grained soils, on the degree of interconnection of the soil particles. Soils dominated by plate-shaped particles are more compressible than those with predominantly spherical granules. Soil in the undisturbed state is less compressible than the same soil in the disturbed state. The soil is realistically neither elastic nor plastic. Appropriate hypotheses of displacement dependence on stress change in granular soils have not been formulated though. However, settlement can be determined by semi-empirical methods (Terzaghi *et al.* 1996).

4.1 Deformations/settlement due to primary compression

The problem of soil consolidation has been explored by many authors around the world over the past century. Several papers have been published on the topic of primary consolidation (Yu and Wu 2013, Nhan *et al.* 2019, Chiaradonna *et al.* 2019). The effects of creep during

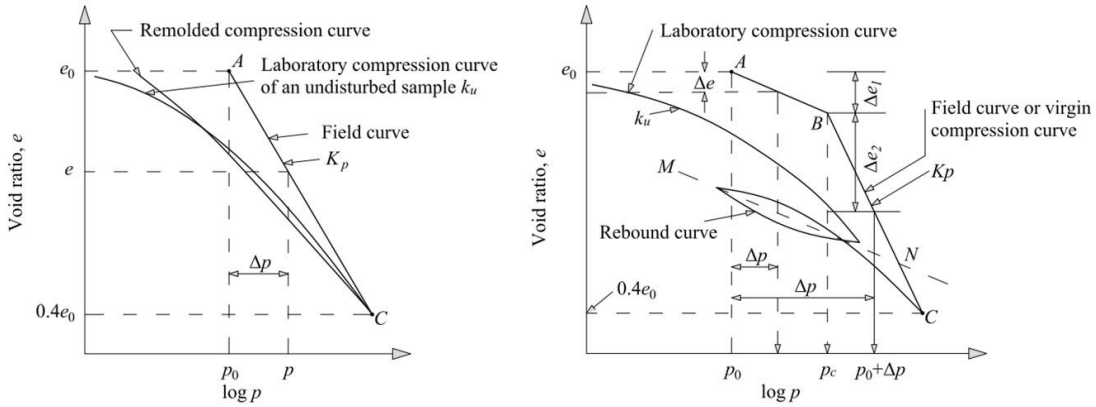

Fig. 4 Characteristic curves from compression test

primary consolidation were studied by Gang Bi *et al.* (2019). Fei Liu *et al.* (2020) analyzed the characteristics of consolidation in complex funding. The parameters of the oedometer curves defined for a given fine-grained soil are generally used to calculate subsidence. Characteristic oedometer curves are shown in Fig. 4.

The slope of the field compression curve K_p on the semi-logarithmic diagram is defined as the compression index C_c (Fig. 4).

The equation for C_c, can be written as

$$C_c = \frac{e_0 - e}{\log p - \log p_0} = \frac{e_0 - e}{\log p / p_0} = \frac{\Delta e}{\log p / p_0} \tag{9}$$

where e_0 is initial void ratio, e is void ratio at the end of primary consolidation, p_0 is stress in natural state, p is consolidation pressure.

Total settlement during primary compression can be written as

$$S_t = H_i \cdot \frac{C_c}{1+e_0} \cdot \log \frac{p_0 + \Delta p}{p_0} \tag{10}$$

where H is the thickness of the layer susceptible to consolidation, and the index i refers to the individual layers in the multilayer substrate exposed to consolidation. The calculation of settlement depends on whether the additional stress from the load on the soil surface Δp is less or higher than the natural stress p_0. In the case of overconsolidated soils (field curve given in Fig. 4), the settlement caused by the load for which states that $p_0+\Delta p \leq p_c$, is calculated as

$$S_t = \frac{C_s \cdot H}{1+e_0} \cdot \log \frac{p_0 + \Delta p}{p_0} \tag{11}$$

where C_s represents the slope of the field curve on part AB called the swelling coefficient.

In case the stresses from applied load are higher than the preconsolidation stress, the slopes of both parts (AB and BC) of the curve, given in Fig. 4, should be included for the settlement calculation. Now the settlement equation S_t can be written using Eqs. (10) and (11), as

$$S_t = \frac{C_s \cdot H}{1+e_0} \cdot \log \frac{p_c}{p_0} + \frac{C_c \cdot H}{1+e_0} \cdot \log \frac{p_0 + \Delta p}{p_c} \tag{12}$$

The following value can be adopted for the swelling coefficient: $C_s \approx$ (1/5-1/10)C_c. Thanks to the results of extensive tests around the world, the values of the compression index C_c can be expressed as a function of certain soil parameters, (Skempton 1944, Terzaghi and Peck 1948, Azzouz *et al.* 1976, Hough 1957, Nagarah and Murthy 1985).

4.2 Deformations / settlement due to secondary compression

Depending on the characteristics of the soil on which the pavement structure is placed, the effects of secondary compression expressed through settlement (rutting) of the pavement structure can be expected. The secondary weather effects in the soil are a phenomenon analogous to the creep of other overloaded materials in the plastic state. Delayed progressive sliding of solid soil particles against each other during their adjustment ("positioning") in the compaction process is probably responsible for a secondary weather effects. If the measure of plastic deformation of individual soil particles and their sliding on each other is slower than the measure of pore volume reduction, then secondary time effects prevail, which is reflected in the form of a compression-time curve. All factors affecting the measure of secondary soil compression are still insufficiently investigated. There are also no satisfactory methods for reliable analyzes and predictions of these effects.

Secondary soil compressibility has been studied in the past century by several researchers around the world. Toshihiko Takeda *et al.* (2012) investigated the level of secondary consolidation during the time of primary consolidation in the oedometric experiment. Matchala Suneel *et al.* (2017) proposed a simple equation for defining the secondary compression index for clay soils as a function of pore coefficient. Nan Jiang *et al.* (2020) studied the influence of soil structure and yield strength on the secondary compression coefficient of soil, during loading under laboratory conditions. Hong *et al.* (2012) analyzed the compressibility of natural and disturbed clays. Józefiak and Zbiciak (2017) dealt with modelling of secondary consolidation in soil mechanics, using rheological schemes. Secondary consolidation was investigated by Vladimir

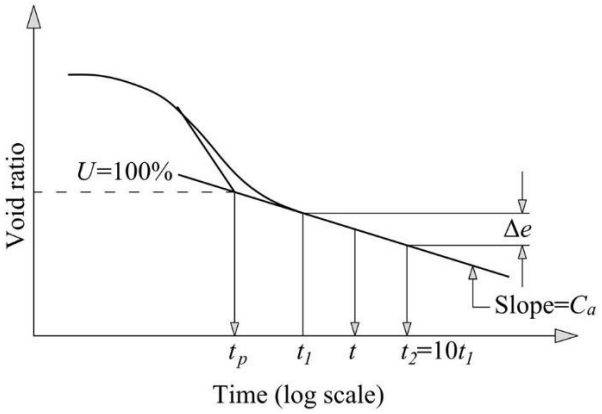

Fig. 5 The *e*-log*t* curve for a given load, which represents the secondary compression

Kapustin *et al.* (2017). Jieqing Huang *et al.* (2014) derived the finite consolidation equation taking into account nonlinear compressibility, nonlinear soil permeability, on soft clays using the finite element method. Tewatia (2012) dealt with the trends of primary and secondary consolidation of compressible soil. Hamed *et al.* (2021) investigated the consolidation (primary and secondary) behaviors of organic soil depending on the water content in the soil. The measure of secondary compression can be expressed in terms of the secondary compression coefficient C_a, shown by Eq. (13)

$$\frac{C_a}{1+e_0}=\frac{\Delta e}{1+e_0}\cdot\frac{1}{\log(t_2-t_1)} \quad \rightarrow \quad \Delta e = C_a\cdot\log\frac{t_2}{t_1} \tag{13}$$

where C_a is the slope of the linear part of *e*-log*t* curve, known as the secondary compression coefficient, Fig. 5.

Secondary compression is expressed by a decrease of the pore coefficient over time, normalized to the duration of the primary compression phase. The general term for settlement due to secondary compression under final load can be expressed as

$$S_s=\frac{\Delta e}{1+e_0}\cdot H \tag{14}$$

The value of Δe, measured in the interval from t/t_p=1 to any time t, can be determined from the curve e-t/t_p which corresponds to the final pressure.

Substituting Δe from Eq. (13), as well as for the constant value of C_a between t_p and t, Eq. (14) becomes

$$S_s=\frac{C_a}{1+e_0}\cdot H\cdot\log\frac{t}{t_p} \tag{15}$$

where e_0 is the initial void ratio, t_p is the time of duration of primary consolidation, H is the thickness of the compressible soil layer, T is any time of load duration.

The effects of various factors that affect the secondary compression have not been sufficiently investigated, and the secondary compression coefficient cannot be accepted with great reliability. As a recommendation for defining the secondary compression coefficient, the diagrams and tables of the authors who investigated the effects of secondary compression are given. Mesri and Godlewski (1977) conclude that for any soil the C_a/C_c ratio is constant (where C_c is the primary compression coefficient (index)). The value of the C_a/C_c ratio for some geotechnical materials according to Terzaghi *et al.* (1996) ranges from 0.01 to 0.07.

5. Analysis of the stress-strain state of the geo-substrate for traffic loads

Pavement structures, according to the valid procedures, are designed to the traffic load defined by the number of transitions of equivalent axle load 82 *kN* (100 *kN*) in the designed period. Design is performed using the usual procedures through adopted nomograms, tables, etc. Recently, design has been carried out in the first step by adopting the geometry and materialization of the pavement structure using nomograms and tables, and in the second step the stress - strain state at the characteristic cross-sectional points of the pavement structure is checked for the adopted pavement structure.

It should be emphasized that the nomograms and tables are derived on the basis of the AASHTO Road Test, on different geometries and materialization of pavement structures, at vehicle speeds of 56 *km*/*h*. It is evident that on the parts of the roads, where the permitted vehicle speeds are lower than stated (56 *km*/*h*), the deformations on the road structure (rutting) are significantly higher if the speeds are lower. This led the authors of this paper to include secondary settlement effects and creep effects of the material under constant load in the pavement structure analyzes. The idea is that the settlement (deformation) achieved through the effects of secondary compression and creep is achieved at the time of reaching the primary compression, which is common to occur during the time of road construction. It is concluded that the mentioned effects of secondary compression and creep could be included in design of pavement structures, applying additional load in relation to the one defined through the number of equivalent axle loads for the design period of the road. The additional load will also be defined by the number of equivalent axle loads. In order to keep the existing procedures in design of road structures, the authors of this paper predict that the additional load is analyzed as a single load in a way that the

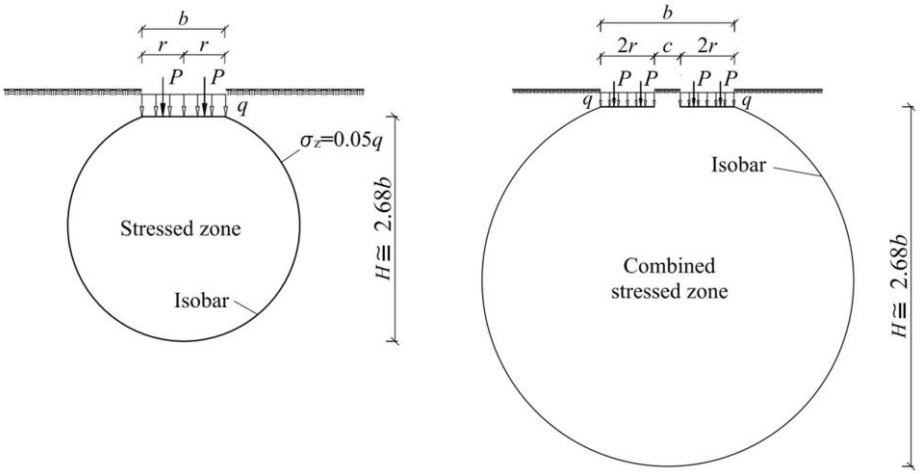

Fig. 6 Distribution of pressure stresses by depth below the load on the surface of the half-space

defined traffic load, according to current procedures, is corrected with correction factor (K_K) as a function of traffic speed.

Defininig of the correction coefficient, K_K, is shown below. The stress-strain state under the tires is analyzed Fig. 6. The analysis is performed for a homogeneous geoenvironment. In the case of a layered medium, a similar analysis for all layers or an analysis of a homogenic medium with equivalent compression coefficients is possible. The following variables were included in the analysis: depth of impact (H), natural stress state (p_0), contact surface of tires and road construction (A_k), tire load (p), natural pore coefficient (e_0), primary compression coefficient (C_C), secondary compression coefficient (C_S), primary compression time (t_p), load duration (t), traffic load (number of equivalent axle loads in design time) (N).

The radius of load influence (r) depends, in addition to the load (P), on the pressure in the tires (q) and is given by the following expression

$$r = \sqrt{\frac{P}{\pi \cdot q}} \tag{16}$$

The natural stress at half the depth of influence is given by Eq. (17)

$$p_0 = h \cdot \gamma \ [kPa] \tag{17}$$

where h is half of height of the impact H. The stress from the traffic load on the contact surface is given by Eq. (18)

$$p = \frac{50}{A_k} \ [kPa] \tag{18}$$

where $A_k = r^2 \cdot \pi \ [m^2]$ is the contact surface of the tire and road, and r is the radius of the contact surface.

The increase in stress at half the height of impact (H) from the traffic load is given by Eq. (19)

$$\Delta p' = p\left(1 - \frac{h^3}{(h^2 + r^2)^{3/2}}\right) \tag{19}$$

The compression coefficient can be represented by the natural pore coefficient as C_c=0.39·e_0, where is e_0- pore coefficient in the natural state.

The time where the primary compression is completed, given the vehicle speed of 56 *km/h* can be shown by Eq. (20)

$$t_p = 0.0193 \cdot N \ [\text{sec}] \tag{20}$$

where N is number of equivalent axle loads for design period of the road. Settlement (deformation) due to primary compression is given by Eq. (21)

$$S_c = \frac{C_c \cdot H}{1 + e_0} \cdot \log \frac{p_0 + \Delta p'}{p_0} \tag{21}$$

The secondary compression coefficient can be expressed in terms of the primary compression coefficient, Eq. (22)

$$C_a = 0.04 \cdot C_c \tag{22}$$

Secondary settlement (deformation) can be calculated using Eq. (23)

$$S_s = \frac{C_a \cdot H}{1 + e_0} \cdot \log \frac{t}{t_p} \tag{23}$$

The total settlement can be determined using Eq. (24)

$$S = S_c + S_s = \frac{C_c \cdot H}{1 + e_0} \cdot \log \frac{p_0 + \Delta p'}{p_0} + \frac{C_a \cdot H}{1 + e_0} \cdot \log \frac{t}{t_p} \tag{24}$$

When designing the pavement structure, it is necessary to meet the requirement that the total settlement is completed in the time of primary compression, ie. during the construction period. Therefore, the stress level will be required, which will lead to the total settlemene being completed during the construction of the road, ie. at the time of primary compression. We will get the stress level from Eq. (25)

$$S = \frac{e_0 H \left(0.027 + 0.0068 \log(t) + 0.169 \log \left(1 + \frac{2\left(50 - \frac{50H^3}{\left(H^2 + 4r^2\right)^{3/2}} \right)}{H \pi r^2 \gamma} \right) \right)}{1 + e_0} \tag{25}$$

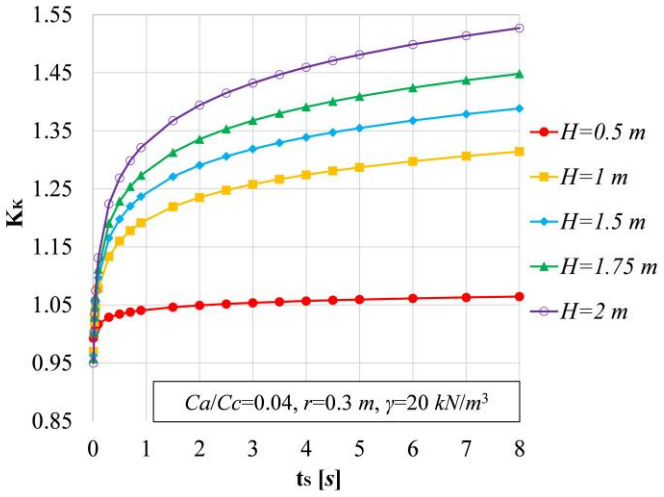

Fig. 7 Correction coefficient of traffic load as a function of stopping time for different depths of impact

Table 1 Corection coefficient of traffic load as a function of stopping time for different depths of impact

t_S [s]	0.2	0.6	1.0	2.0	3.0	4.0	5.0	6.0	7.0	8.0
H [m]	K_K									
0.50	1.025	1.036	1.042	1.049	1.054	1.057	1.059	1.061	1.063	1.065
1.00	1.113	1.170	1.197	1.235	1.258	1.274	1.287	1.298	1.307	1.314
1.50	1.139	1.210	1.244	1.291	1.319	1.339	1.355	1.368	1.379	1.388
1.75	1.161	1.242	1.281	1.335	1.368	1.391	1.409	1.424	1.437	1.448
2.00	1.189	1.284	1.331	1.394	1.432	1.460	1.481	1.499	1.514	1.527

It follows

$$\Delta p = 0.586 H\gamma\left(-0.854 + t^{0.04}\left(1 + \frac{2\left(50 - \frac{50H^3}{\left(H^2+4r^2\right)^{3/2}}\right)}{H\pi r^2\gamma}\right)\right) \quad (26)$$

Based on Eq. (25) as well as Eq. (19) and Eq. (26), it follows that the correction coefficient (K_K) of the traffic load can be expressed as

$$K_K = \frac{183.949 Hr^2\gamma\left(-0.854 + t^{0.04}\left(1 + \frac{2\left(50 - \frac{50H^3}{\left(H^2+4r^2\right)^{3/2}}\right)}{H\pi r^2\gamma}\right)\right)}{50 - \frac{50H^3}{\left(H^2+4r^2\right)^{3/2}}} \quad (27)$$

As an example, for road locations such as intersections where vehicles stop, the previous equations, as a function of stopping time (t_s), can be written in the form given by Eqs. (28)-(30). The following, during stopping time (t_s), expressed as the total stopping time (design number of standard axle-N transitions included), $t_s = t{\cdot}N$, and for specific values: H=1.5 m, r=0.3 m, γ= 20 kN/m^3, e_0=0.58, the previous equations can be written as

$$S = 0.1276 + 0.0037\log(t) \quad (28)$$

$$\Delta p = -15 + 58.898 t^{0.04} \quad (29)$$

$$K_K = \frac{\Delta p}{\Delta p'} = -42.499 + 166.874 t^{0.04} \quad (30)$$

In Fig. 7 and Table 1, the value of the correction coefficient of traffic load as a function of stopping time for different values of the depth of impact (as a function of tire dimensions) is given, at constant other values.

For values of the depth of impact (H) that are not shown on the curves (Fig. 7) and in Table 1, the interpolation procedure should be used.

Fig. 8 and Table 2 show the values of the traffic load correction coefficient as a function of the stopping time for different values of the ratio of the secondary and primary compression coefficients at constant other variables.

For the values of the ratios of the secondary and primary compression coefficients that are not shown on the curves (Fig. 8) and Table 2, interpolation procedure should be used.

In situations of driving speeds limitation, which are less than the reference speed (approx. 56 km/h) applied in the AASHTO experiment, it is necessary to correct the traffic load by the traffic load correction coefficient defined as a function of vehicle speed. The traffic load correction

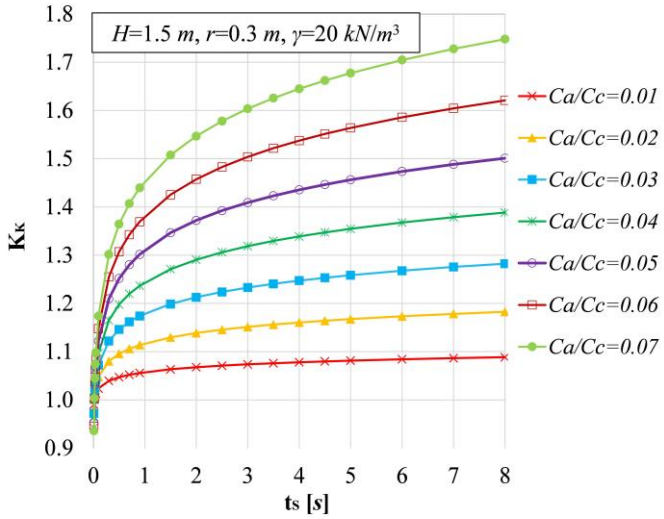

Fig. 8 Traffic load correction coefficients as a function of stopping time for different values of the ratio of secondary and primary compression coefficients

Table 2 Traffic load correction coefficients as a function of stopping time for different values of the ratio of secondary and primary compression coefficients

$t_S[s]$	0.2	0.6	1.0	2.0	3.0	4.0	5.0	6.0	7.0	8.0
C_a/C_c						K_K				
0.01	1.034	1.050	1.057	1.068	1.074	1.078	1.081	1.084	1.087	1.088
0.02	1.068	1.101	1.117	1.139	1.151	1.160	1.168	1.173	1.178	1.183
0.03	1.104	1.155	1.179	1.213	1.233	1.247	1.259	1.268	1.276	1.282
0.04	1.140	1.210	1.244	1.291	1.319	1.339	1.355	1.368	1.379	1.388
0.05	1.177	1.267	1.311	1.372	1.409	1.436	1.456	1.474	1.488	1.501
0.06	1.215	1.326	1.381	1.458	1.504	1.537	1.564	1.586	1.604	1.621
0.07	1.253	1.388	1.454	1.547	1.604	1.645	1.678	1.705	1.728	1.748

coefficient is defined by Eq. (33). The retention/crossing time of a part of the road for specific speed of vehicle movement (less than representative) is shown, by the approach of proportionality in relation to the representative speed, for the total (designed) number of crossings of standard axles. A representative speed in analyzes, was the adopted speed applied in the conducted AASHTO tests of 56 *km/h*. Therefore, the retention / transition time at lower speeds can be defined as t_S=0.3·3.6·*N*/*V*. For the time defined in this way, the derivation of the expression for the traffic load correction coefficient follows Eq. (33).

$$S=\frac{e_0 H\left(0.027+0.0068\log(\frac{1}{V})+0.169\log\left(1+\frac{2\left(50-\frac{50H^3}{\left(H^2+4r^2\right)^{3/2}}\right)}{H\pi r^2\gamma}\right)\right)}{1+e_0} \tag{31}$$

$$\Delta p=0.587H\gamma\left(-0.851+\left(\frac{1}{V}\right)^{0.04}\left(1+\frac{2\left(50-\frac{50H^3}{\left(H^2+4r^2\right)^{3/2}}\right)}{H\pi r^2\gamma}\right)\right) \tag{32}$$

$$K_K=\frac{184.516Hr^2\gamma\left(-0.851+\left(\frac{1}{V}\right)^{0.040.04}\left(1+\frac{2\left(50-\frac{50H^3}{\left(H^2+4r^2\right)^{3/2}}\right)}{H\pi r^2\gamma}\right)\right)}{50-\frac{50H^3}{\left(H^2+4r^2\right)^{3/2}}} \tag{33}$$

For specific values: H=1.5 *m*, r=0.3 *m*, γ=20 *kN/m*^{3}, e_0=0.58, Eqs. (31)-(33) become

$$S=0.1278+0.0033\log(\frac{1}{V}) \tag{34}$$

$$\Delta p=-15+59.08\left(\frac{1}{V}\right)^{0.04} \tag{35}$$

$$K_K=\frac{\Delta p}{\Delta p'}=-42.499+167.389\left(\frac{1}{V}\right)^{0.04} \tag{36}$$

In Fig. 9 and Table 3, the value of the traffic load correction coefficient as a function of vehicle speed for different values of impact depth (as a function of tire dimensions) is given, with constant other values shown in the figure.

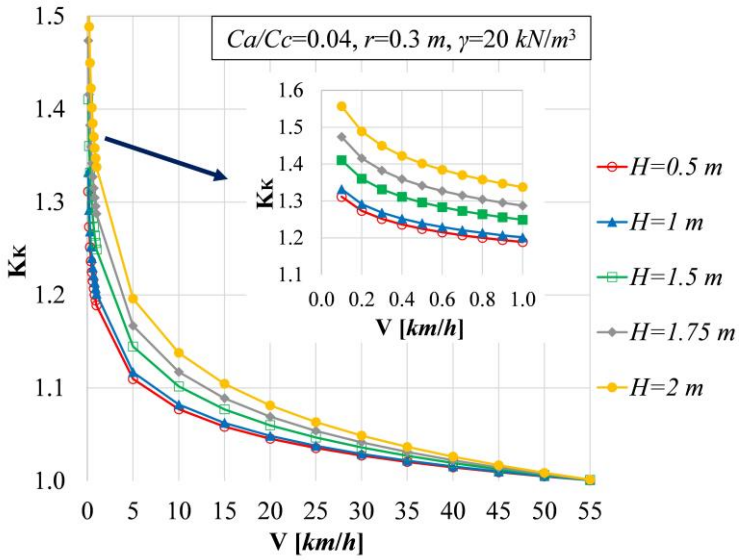

Fig. 9 Traffic load correction coefficient as a function of vehicle speed, for different depths of impact (H)

Table 3 Traffic load correction coefficient as a function of vehicle speed for different depths of impact (H)

V [km/h]	0.1	2.0	5.0	10.0	15.0	20.0	25.0	35.0	45.0	55.0
H [m]						K_K				
0.50	1.299	1.148	1.105	1.074	1.056	1.044	1.034	1.020	1.009	1.001
1.00	1.332	1.164	1.117	1.082	1.062	1.048	1.038	1.022	1.010	1.001
1.50	1.410	1.203	1.145	1.101	1.077	1.059	1.047	1.027	1.012	1.001
1.75	1.474	1.234	1.167	1.117	1.089	1.069	1.054	1.031	1.014	1.001
2.00	1.557	1.275	1.196	1.138	1.105	1.081	1.063	1.037	1.017	1.001

Table 4 Traffic load correction coefficient as a function of vehicle speed, for different values of secondary and primary compression coefficient ratios

V [km/h]	0.1	2.0	5.0	10.0	15.0	20.0	25.0	35.0	45.0	55.0
C_a/C_c						K_K				
0.01	1.093	1.048	1.035	1.025	1.019	1.015	1.012	1.007	1.003	1.000
0.02	1.192	1.098	1.071	1.050	1.038	1.030	1.023	1.013	1.006	1.000
0.03	1.298	1.150	1.107	1.076	1.057	1.045	1.035	1.020	1.009	1.001
0.04	1.410	1.203	1.145	1.102	1.077	1.060	1.047	1.027	1.012	1.001
0.05	1.530	1.258	1.183	1.128	1.097	1.075	1.059	1.034	1.016	1.001
0.06	1.658	1.315	1.222	1.155	1.117	1.091	1.071	1.041	1.019	1.001
0.07	1.794	1.374	1.262	1.183	1.138	1.106	1.083	1.048	1.022	1.002

For values of the depth of impact (H) that are not shown at the curves Fig. 9 and in Table 3, interpolation procedure should be used.

Fig. 10 and Table 4 show the traffic load correction coefficient as a function of vehicle speed for different values of the ratio of secondary and primary compression coefficients, at constant values of other variables shown in the figure.

For the values of the ratios of the secondary and primary compression coefficients that are not shown on the curves Fig. 10 and Table 4, interpolation procedure should be used.

6. Conclusions

- Deformations of the constructed flexible pavement structures indicate shortcomings (omissions/lapse) in the approach of their dimensioning.
- Deformation of settlement (subsidence)/ruts are mainly pronounced on sections of roads where vehicle speeds are reduced and on the vehicle stopping points, such as intersections. For short road sections, the functional dependence of the realized deformations with the speed of traffic can

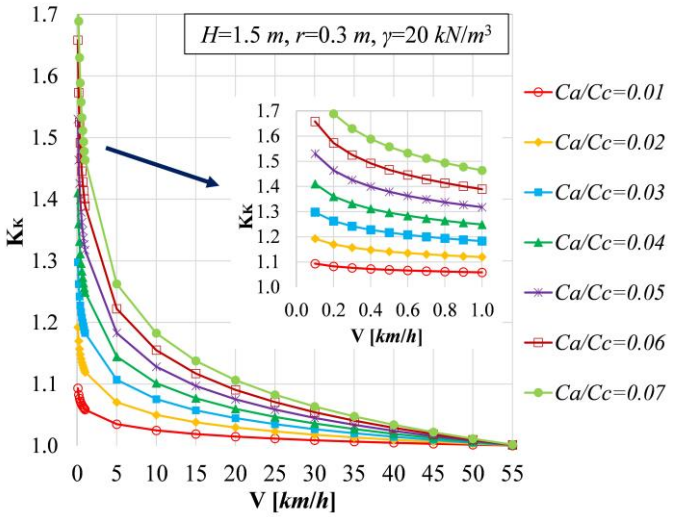

Fig. 10 Traffic load correction coefficient as a function of vehicle speed, for different values of the ratio of secondary and primary compression coefficients

be established with great reliability. Namely, for such short sections, all other factors that can potentially lead to deformations can be considered unchangeable.

- Deformations in the form of ruts on the surfaces of flexible pavement structures can be caused by deformation of bound asphalt layers or unbound geomechanical layers, including natural soil layers on which the road is built. By analyzing the shape of the deformation of the road surface, a conclusion can be drawn about the dominant factors that influenced the resulting deformation. In this paper, the authors only dealt with the problem of deformation of the geotechnical environment over time, and how to overcome them, using existing project procedures in the dimensioning of flexible pavement structures. The defined traffic load correction coefficient, as one of the influences on which the flexible traffic structure is dimensioned, is applied in the budget analyzes to all layers of the pavement structure, and thus will have a positive effect on the dimensioning of bound asphalt layers, which were not analyzed in this work.
- Deformability of flexible pavement structures during exploitation indicates a geotechnical problem of secondary settlement (subsidence) of granular layers of pavement structure and geo-substrate/subgrade.
- Pavement structures, according to current procedures, are dimensioned for traffic load defined by the number of crossings of equivalent axles 82 *kN* (100 *kN*) in the projected period of exploatation of road. Patterns, diagrams, according to which flexible rutting constructions are dimensioned, are defined on the basis of carried extensive research (AASHTO Road Test) at vehicle speeds of approximately 56.0 *km/h*.
- The analysis of deformations concludes that the level of deformation of flexible pavement structures is a function of the speed of traffic.
- The authors defined the traffic load correction coefficient, which would be applied to the already determined number of traffic axles (according to established procedures) for traffic speeds less than 56.0 *km/h*, as well as in situations where traffic jams are predicted, such as intersections.
- Correction coefficient (K_K), is presented in the form of expressions, diagrams and tables in the paper. The analysis is performed for a homogeneous geoenvironment. In the case of a layered medium, a similar analysis for all layers or an analysis of a homogenic medium with equivalent compression coefficients is possible.
- It should be emphasized that the effects of various factors, which affect the secondary compression, are still insufficiently investigated, and the secondary compression coefficient/index cannot be accepted with great reliability. Recommendations for defining the secondary compression coefficient were used in this paper. Research in order to establish a more reliable dependence of secondary compression and creep as a function of various factors, is imposed as an imperative requirement in order to confirm the proposed dependences for the defined correction factor (K_K) of traffic load.

References

AASHTO (1972), *AASHTO Interim Guide for Design of Pavement Structures*, American Association of State Highway and Transportation Officials; Washington D.C., USA.

Babić, B. (1997), *Projektiranje Kolničkih Konstrukcija*, Hrvatsko društvo građevinskih inženjera, Zagreb, Hrvatska.

Bi, G., Ni, S., Wang, D., Chen, Y., Wei, J. and Gong, W. (2019),

"Creep in primary consolidation with rate of loading approach", *Scientific Reports*, 9:8992. https://doi.org/10.1038/s41598-019-45498-0

Boler, H., Mishra, D., Hou, W. and Tutumluer, E. (2018), "Understanding track substructure behavior: Field instrumentation data analysis and development of numerical models", *Civil Engineering Faculty Publications and Presentation, Department of Civil Engineering.*

Burmister, D.M. (1943), "The theory of stresses and displacements in layered systems and applications to the design of airport runways", *Proceedings of the 23rd Annual Meeting of the Highway Research Board*, Chicago, Illinois, USA, November.

Burmister, D.M. (1945), "The general theory of stresses and displacements in layered soil systems", *J. Appl. Phys.*, **16**(5). https://doi.org/10.1063/1.1707558.

Chiaradonna A., d'Onofrio, A. and Bilotta, E. (2019), "Assesment of post-liquefaction consolidation settlement", *Bull. Earthq. Eng.*. https://doi.org/10.1007/s10518-019-00695-0.

Chou, Y.T. and Larew, H.G. (1969), "Stresses and displacements in viscoelastic pavement systems under a moving load", *Highway Research Record*, **282**, 25-40.

Cvetanović, A. and Banić, B. (2007), *Kolovozne Konstrukcije*, Akademska misao, Beograd, Srbija.

De Beer, M., Maina, J.W., van Rensburg, Y. and Greben, J.M. (2012), "Toward using tire-road contact stresses in pavement design and analysis", *Tire Sci. Technol.*, **40**(4), 246-271. https://doi.org/10.2346/tire.12.400403.

Elliot, J.F and Moavenzadeh, F. (1971), "Analysis of stresses and displacements in three-layer viscoelastic systems", *Highway Research Record*, 345, 45-57.

Gomes Correla, A. and Ramos, A. (2021), "A geomechanics classification for the rating of railroad subgrade performance", *Railway Eng. Sci*., https://doi.org/10.1007/s40534-021-00260-z

Hamed, M., Canakci, H. and Georgees, R.N. (2021), "Experimental investigation on the primary and secondary consolidation behaviours of organic soilunder different water contents", *Arabian J. Geosci.*, 14:2865. https://doi.org/10.1007/s12517-021-09231-4.

Hong, Z.S., Zeng, L.L., Cui, Y.J., Cai, Y.Q. and Lin, C. (2012), "Compression behaviour of natural and reconstituted clays", *Geotechnique*, **62**(4), 291-301. http://dx.doi.org/10.1680/geot.10.P.046.

Huang, J., Xie, X., Zhang, J., Li, J. and Wang, W. (2014), "Nonlinear finite strain consolidation analysis with secondary consolidation behaviour", *Math. Problem. Eng.*, https://doi.org/10.1155/2014/979380.

Huang, Y.H. (1967), "Stresses and displacements in viscoelastic layered systems under circular loaded areas", *Proceedings of the 2nd International Conference on the Structural Design of Asphalt Pavements*, Ann Arbor, MI, USA, August.

Huang, Y.H. (1968a), "Stresses and displacements in nonlinear soil media", *J. Soil Mech. Found. Division*, **94**, 1-19. https://doi.org/10.1061/JSFEAQ.0001079.

Huang, Y.H. (1973b), "Stresses and strains in viscoelastic multilayer systems subjected to moving loads", *Highway Research Record*, **457**, 60-71.

Huang, Y.H. (1993), *Pavement Analysis and Design*, Prentice Hall, Upper Saddle River, NJ, USA.

Huhtala, M., Pihlajamäki, J. and Pienimäki, M. (1989), "Effects of tires and tire pressures on road pavements", *T. Res. Record*, **1227**, 107-114.

Jiang, N., Wang, C., Wu, Q. and Li, S. (2020), "Influence of structure and liquid limit on the secondary compressibility of soft soils", *J. Mar. Sci. Eng.*, **627**(8), 195-208. https://doi.org/10.3390/jmse8090627.

Jozefiak, K. and Zbiciak, A. (2017), "Secondary consolidation modelling by using rheological schemes", *MATEC Web of Conferences*, 117. https://doi.org/10.1051/matecconf/20171170006.

Kapustin, V., Khaustov, V. and Kapustin, V.K. (2017), "Researches of soilses secondary consolidation", *iipp*, **451**, 339-344. https://doi.org/10.5937/jaes15-14652.

Kim, M., Tutumluer, E. and Kwon, J. (2009), "Nonlinear pavement foundation modeling for three-dimensional finite-element analysis of flexible pavements", *Int. J. Geomech.*, (9), 195-208. https://doi.org/10.1061/ASCE1532-364120099:5195.

Le, T.M., Fatahi, B., Disfani, M. and Khabbaz, H. (2015), "Analyzing consolidation data to obtain elastic viscoplastic parameters of clay", *Geomech. Eng.*, **4**(8), 559-594. https://doi.org/10.12989/gae.2015.8.4.559.

Liu, F., Qin, K. and Han, Y. (2020), "Simplified method for consolidation settlement calculation of combined composite foundation", *Shock Vib.*, 2020. https://doi.org/10.1155/2020/8818161

Mesri, G. and Godlewski, P.M. (1977), "Time and stress-compressibility interrelationship", *J. Geotech. Eng. Division*, **103**(5), 417-430. https://doi.org/10.1061/AJGEB6.0000421.

Nhan, T.T., Nhat, P.C., Huong, H.T.S., Thach, T.X., Thien, D.Q. and Nhan, N.T.T. (2019), "Time to the end of primary consolidation (EOP) of soft clayey soils: concerning the effect of Atterberg's limit and cyclic loading history", *Hue University J. Sci. Techniques and Technology*, **2**(128), 29-41. https://doi.org/10.26459/hueuni-jtt.v128i2A.5424.

Pascale, P., Doré, G. and Prophète, F. (2011), "Characterization of tire impact on the pavement behaviour", *Can. J. Civil Eng.*, **31**(5), 860-869. https://cdnsciencepub.com/doi/10.1139/l04-038.

Perloff, W.H. and Moavenzadeh, F. (1967), "Deflection of viscoelastic medium due to moving loads", *Proceedings of the 2nd International Conference on the Structural Design of Asphalt Pavements*, Ann Arbor, MI, USA, January.

Rashidi, M., Azadeh, S., Fatehirad, P., Emadi, S.M. and Lotfi-Aski, A. (2013), "Prediction of bias-ply tire deflection based on contact area index, inflation pressure and vertical load using linear regression model", *World Appl. Sci. J.*, **22**(7), 911-918. https://doi.org/10.5829/idosi.wasj.2013.22.07.2997.

Schulz-Poblete, M.V., Johannes Grabe, P. and Wilem Jacobsz, S. (2018), "The influence of soil suctions on the deformation characteristics of railway formation materials", *Transportation Geotechnics*. https://doi.org/10.1016/j.trgeo.2018.11.006.

Shayesteh, A., Ghasemisalehabadi, E., Khordehbinan, M.W. and Rostami, T. (2017), "Finite element method in statistical analysis of flexible pavement", *J. Mar. Sci. Technol.*, **25**(2), 142-152. https://doi.org/10.6119/JMST-016-0721-1.

Suneel, M., Konni, G.R., Chul, I.J. and Dung, N.T. (2017), "Secondary compression index equation for soft clays", *Geotech. Geol. Eng*., https://doi.org/10.1007/s10706-017-0358-x.

Takeda, T., Sugiyama, M., Akaishi, M. and Chang, H.W. (2012), "Secondary compression behaviour in one-dimensional consolidation test", *J. Geoeng.*, **2**(7), 53-58.

Terzaghi, K., Peck, R.B. and Mesri, G. (1996), *Soil Mechanics in Engineering Practice – 3rd Ed.*, John Wiley & Sons, Inc., New York, NY, USA.

Tewatia, S.K. (2012), "Trend of settlement in primary and secondary consolidations", *Geomech. Geoeng. Int. J*., 1-10. https://doi.org/10.1080/17486025.2012.698023.

Ullidtz, P. (1997), "Modelling flexible pavement response and performance - instructor notes on nondestructive pavement analysis for Pre-Conference Technical Series", *Proceedings of the 8th International Conference on Asphalt Pavements*, Seattle, WA, USA, August.

Yu, J.Q. and Wu, X.W. (2013), "Analysis of the primary consolidation settlement considering of the settlement load", *Appl. Mech. Mater.*, 353-356, 1063-1066.

https://doi.org/10.4028/www.scientific.net/AMM.353-356.1063.

JS